IEEE Access
Multidisciplinary ⋮ Rapid Review ⋮ Open Access Journal

Received 20 June 2024, accepted 6 July 2024, date of publication 12 July 2024, date of current version 29 July 2024.

Digital Object Identifier 10.1109/ACCESS.2024.3427402

RESEARCH ARTICLE

Optimizing Nominal Current Output for Aeronautical Ground Lighting Using Machine Learning and Meteorological Data

W. M. R. JAMALUDIN[1], N. H. NIK ALI[2], (Senior Member, IEEE), W. M. WAN MOHAMED[1], AND N. A. M. ISA[3]

[1]School of Mechanical Engineering, College of Engineering, Universiti Teknologi MARA, Shah Alam, Selangor 40450, Malaysia
[2]School of Electrical Engineering, College of Engineering, Universiti Teknologi MARA, Shah Alam, Selangor 40450, Malaysia
[3]Technical Services Division, Malaysia Airports Holdings Berhad, Malaysia Airports Sepang, Sepang, Selangor 64000, Malaysia

Corresponding author: N. H. Nik Ali (hakimiali@uitm.edu.my)

This research article was financially supported by Universiti Teknologi MARA and Institute of Postgraduate Studies UiTM.

ABSTRACT Although there have been numerous studies on visibility prediction, there have been insignificant studies conducted to predict nominal current output based on visibility. Therefore, this study focuses on optimizing nominal current output at Subang Airport by employing artificial intelligence and meteorological data. The research leverages daily meteorological data to enhance visibility prediction and address aeronautical ground lighting issues emphasizing on the runway edge light. The methodology involves a three-step modeling approach with Bayesian optimization. First, Gaussian Process Regression was utilized to predict visibility, incorporating various meteorological parameters. Second, a correction filter refines the predictions, integrating models such as Regression Trees, Support Vector Machines, Ensemble of Trees, Neural Networks, and Gaussian Process Regression. Finally, prediction of nominal output current was conducted using error squared, generated from the correction filter, and time. Various machine learning models, including Decision Trees, Discriminant Analysis, Naïve Bayes Classifiers, Support Vector Machines, Nearest Neighbor Classifiers, Ensemble Classifiers, and Neural Network Classifiers were evaluated to determine the most effective model. Cross-fold validation with a 5-fold split ensures the reliability and precision of the machine learning algorithms. Performance metrics such as Mean Absolute Error, Mean Squared Error, Root Mean Squared Error, and R-squared were used to evaluate the models. Results highlight the stacked model of Gaussian Process Regression, Gaussian Process Regression, and Nearest Neighbor Classifiers as the most accurate, achieving a 96.2 % accuracy in predicting and improving nominal output current. In conclusion, this study has introduced a novel approach to predicting and improving nominal output current for runway edge light utilizing limited historical meteorological data.

INDEX TERMS Aeronautical ground lighting, machine learning, meteorological data, nominal current output.

I. INTRODUCTION

In today's modern era of aviation, the lack of a standard or guidance on the nominal current output in airport operations is becoming a growing concern. This could potentially pose risks to the safety and efficiency of aircraft operations. From the foregoing will be evident the importance of adjusting the intensity of the lights in an aerodrome lighting system according to the prevailing conditions is crucial to achieve optimal results without excessive glare that could disorient the pilot. The appropriate intensity setting will depend on the background brightness and visibility conditions [1].

The associate editor coordinating the review of this manuscript and approving it for publication was Mohammad J. Abdel-Rahman.

Additionally, it is recommended that every country should adapt their intensity setting procedures to ensure optimal lighting intensities [2].

To accurately predict the optimized nominal current output, which is directly related to visibility, it is essential to have a precise prediction of visibility. When it comes to the input variables used for prediction, two types of data are commonly chosen. The first type includes fine particulate matter (PM) and atmospheric aerosol [3], while the second type comprises various meteorological elements that may impact visibility [4], [5]. In terms of prediction methods, artificial intelligence techniques have become increasingly popular in recent years for studying airport visibility [6]. However, there are limited studies on airport visibility prediction due to the challenge of obtaining a large amount of long-term meteorological data and visibility observations around airports [6]. At Sofia Airport, machine learning methods were employed to evaluate visibility by analyzing meteorological factors such as fog stability index, dew point temperature, cloud base, temperature, wind speed, time, pressure, wind direction, and cloud coverage [7]. Additionally, [8] also used meteorological factors to predict visibility in Mondoñedo, Galicia, Spain. The models utilized in their study included Support Vector Machine (SVM), Random Forest (RF), Gaussian Naive Bayes (GNB), K-Nearest Neighbors (KNN), AdaBoost (AB), Gradient Boost (GB), and Multilayer Perceptrons (MLP).

In order to develop reliable forecasting tools for predicting haze in China, [9] collected a comprehensive dataset of meteorological parameters from various monitoring stations across the country. These parameters included wind speed, wind direction, temperature, humidity, and visibility records. Three popular machine learning methods, namely SVM, KNN, and RF, were then employed for visibility forecasting. These methods were chosen due to their established performance in various prediction tasks. In addition, [10] conducted a low visibility prediction at Jay Prakash Narayan International Airport (JPNI) in Patna, India. They used dry bulb temperature, dew point temperature, wind speed, wind direction, relative humidity, and cloud amount to make their predictions. Similarly, [11] conducted a study to predict visibility at six airport stations in the United Arab Emirates. They used meteorological parameters such as air temperature, relative humidity, wind speed, rainfall, sea level pressure, and dew point temperature. They employed Linear Regression (LR), Regression Tree (RT), Ensemble Tree (ET), SVM, GPR, and ANN to predict visibility.

Some researchers also use classification techniques to predict visibility, as shown in [12]. In this study, the authors utilized meteorological parameters including cloud cover, wind direction, wind speed, temperature, pressure, relative humidity, and dew point temperature. They applied various algorithms such as Decision Tree, Linear Discriminant Analysis, Naive Bayes, SVM, KNN, and ANN. Another study conducted by [13] focused on analyzing the persistence and prediction of low-visibility events at Villanubla Airport in Spain during the winter season. In this study, SVM and Extreme Learning Machines (ELM) were employed to forecast visibility. Additionally, [14] developed a visibility estimation model for South Korea using RF, incorporating meteorological parameters. This model successfully provided visibility information in areas where no observations were available.

The summarized literature is presented in Table 1. The table shows that previous studies have contributed to predicting visibility using regression and classification techniques. However, there are limited studies on how to use these methods to determine the optimal nominal current output for aeronautical ground lights. Additionally, it is evident from the table that parameters such as temperature, dew-point temperature, wind speed, wind direction, and pressure are common across all studies. Furthermore, most studies did not apply Bayesian optimization to enhance visibility prediction accuracy.

Therefore, this study utilizes the squared error from visibility prediction along with time and Bayesian optimization to classify the optimum nominal output current. Time is chosen as one of the parameters because it affects the operational aspects of lighting. In actual airport operations, even though the visibility is over 10 000 meters during the day, the lights are switched off. However, during the night when the visibility is more than 10 000 meters, the lights are switched on.

Hence, as shown in Table 1, the purpose of this study is to predict the optimal nominal current output based on visibility and time. The novelty of this study lies in its approach, which includes:

1) The use of an optimum correction filter to improve visibility prediction in a tropical country.
2) Utilizing the error produced by regression models together with time to classify the optimal nominal current output.
3) Assessing and fine-tuning a wide range of relevant regression and classification techniques, and subsequently assembling these machine learning models to create a robust model with high accuracy for predicting the nominal current output.

This study specifically focuses on the operation of runway edge lights at Subang Airport, particularly in relation to the use of nominal current output to ensure aircraft safety. However, it does not include a study on the impact of nominal current consumption on airside safety, airside operations, electrical and aeronautical ground lighting maintenance programs, and the cost of implementing the results. This is due to specific confidentiality issues with stakeholders.

The research paper consists of Section I, which explains the previous studies, problem statements, objectives, scope of work, and limitations. The rest of the paper is organized as follows: Section II presents the methodology used to

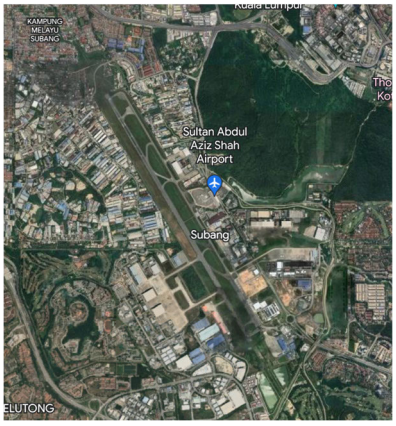

FIGURE 1. Layout of WMSA showing it is situated in the city, surrounded with commercial, residential and buildings with rapid and dense development.

achieve the objectives of this study, Section III describes the results and discussion, and Section IV concludes the overall study.

II. METHODOLOGY

A. STUDY AREA

Subang Airport, as shown in Fig. 1, also known as WMSA in the ICAO Code, is located at 03°07'56" North and 101°33'01" East in Subang, Selangor, Malaysia. It is situated approximately 15 kilometers west of Kuala Lumpur, making it conveniently accessible to both business and leisure travelers. Geographically, WMSA benefits from a favorable climate with consistent weather patterns throughout the year, which makes it an ideal choice for domestic and regional flights. This reliability and convenience to passengers, however, are hampered by an ongoing issue with the airport's aeronautical ground lighting. Currently, halogen fittings are still being used [15], leading to energy wastage. Furthermore, there is no standard or guidance in place for the current consumption of the lighting system in real-time.

To address the issue, daily meteorological data corresponding was collected from the National Oceanic and Atmospheric Administration (NOAA) [16]. Data from April 1st, 2023 until June 30th, 2023 were collected and analyzed. Meteorological factors such as time, daily air temperature, dew point temperature, difference between air temperature and dew point temperature, wind direction, wind speed and pressure were utilized in the calculation and screening processes. The information regarding the collected data can be found in Table 2. The predicted visibility was calculated through modelling, utilizing daily meteorological data. The wind direction is a variable that ranges over a set of degrees. Therefore, it is substituted with the constant numeric representation of 359 degrees to establish a common datum so that it can be read as an integer in MATLAB and visibility exceeding 10 000 meters is replaced with the value of 10 so that a common reference point is obtained to run the regression learner program thus the model could be generalized better.

B. NOMINAL CURRENT

The electrical power for aerodrome ground lighting circuits (series circuit) is typically supplied by constant current regulators (CCRs). This is done to maintain a consistent light output over long distances, such as on aerodrome runways. CCRs are devices specifically designed to provide a steady current output, even when there are variations in input voltage or load resistance. In the aviation industry, it is crucial to maintain consistent lighting conditions for pilots during take-off, landing, and taxiing. Therefore, constant current regulators are used to power runway and taxiway lighting [17]. These regulators are designed to produce a constant current output that remains unaffected by changes in the circuit load or input voltage from the power source. They are also capable of providing two or more output currents when dimming of the lights is required. Based on [17] and the type of CCRs used in Malaysia, the current consumption classification is categorized into 5 steps, as shown in Table 3. These 5 steps are used to select the appropriate intensity, ranging from 2.8 amperes to 6.6 amperes, with a tolerance of ± 0.1 amperes. This selection ensures the safe operation of aircraft under specific atmospheric conditions.

C. K-FOLD CROSS-VALIDATION

A cross-validation method was used to develop every algorithm, regardless of the split in data used for training and evaluating [13], [18]. The fold was set to 5, with a split of 20 % for validation and 80 % for training, in order to prevent overfitting and avoid suboptimal models due to an unbalanced distribution of the dataset [19]. Fig. II illustrates an example of the stacking structure when fold is set to 5. This method proves valuable for evaluating the effectiveness of a machine learning system, offering several benefits. Firstly, it provides a more precise evaluation of algorithm performance compared to training and assessing using a single data split. Secondly, it optimizes data utilization by allowing for the inclusion of all datasets, providing an objective assessment of algorithm performance. Thirdly, the k-fold approach facilitates hyperparameter adjustment, preventing overfitting to the validation set. By adjusting hyperparameters and assessing their effectiveness across each fold, optimal hyperparameters can be selected based on their average performance.

D. OVERFITTING

Overfitting refers to a situation in which a model performs well on training data but poorly on unseen test data [21]. This indicates that the model has learned noise in the training data instead of the underlying patterns. Several factors can contribute to overfitting, including the complexity of the model, such as the number of hyperparameters. When a model becomes too complex, it tends to fit too closely to the

TABLE 1. Summary of previous study and proposed method in this study.

Ref	Location	Independent variable	Dependent variable	Visibility prediction model	Bayesian optimization	Nominal current classification
[7]	Sofia Airport	Fog stability index, dew-point temperature, cloud base, temperature, wind speed, time, pressure, wind direction, cloud coverage	Visibility	i. Random Forest ii. Long Short-Term Memory	No	No
[8]	Galicia, Spain	Accumulated precipitation, air temperature, atmospheric pressure, dew-point temperature, ground temperature, global solar radiation, relative humidity, salinity, wind direction, wind speed	Visibility	i. Support Vector Classifier ii. Random Forest iii. Gaussian Naive Bayes iv. K-Nearest Neighbors v. AdaBoost vi. Gradient Boost vii. Multilayer Perceptrons	No	No
[9]	Shenzhen	Time, wind speed, wind direction, relative humidity, temperature	Visibility	i. Support Vector Machine ii. Random Forest iii. K-Nearest Neighbors	No	No
[10]	Jay Prakash Narayan International Airport	Dry bulb temperature, dew-point temperature, wind speed, wind direction, relative humidity, cloud amount	Fog	i. Artificial Neural Network ii. Gradient Boosting Machine iii. Extremely Randomized Tree iv. Extreme Gradient Boosting v. Discrete Random Forest vi. Generalized Linear Models	No	No
[11]	Airports in United Arab Emirates	Temperature, relative humidity, wind speed, rainfall, pressure, dew-point temperature	Visibility	i. Linear Regression ii. Regression Trees iii. Ensemble Trees iv. Support Vector Machine v. Gaussian Process Regression vi. Artificial Neural Network	No	No
[12]	Chengdu	Total cloud cover, low cloud cover, wind direction, wind speed, temperature, humidity, vapor pressure, dew-point temperature, atmospheric pressure	Visibility	i. Decision Tree ii. Linear Discriminant Analysis iii. Naive Bayes iv. Support Vector Machine v. K-Nearest Neighbors vi. Artificial Neural Network	No	No
[13]	Villanubla Airport, Spain	Temperature, relative humidity, wind speed, wind direction, atmospheric pressure	Visibility	i. Support Vector Machines ii. Extreme-Learning Machines iii. Markov Chain Model iv. Mixture of Experts	No	No
[14]	South Korea	Temperature, pressure, wind speed, relative humidity, precipitation	Visibility	Random Forest	No	No
Proposed method in this study		Temperature, dew-point temperature, difference between temperature and dew-point temperature, pressure, wind speed, wind direction	Visibility	i. Regression Trees iii. Ensemble Trees iv. Support Vector Machine v. Gaussian Process Regression vi. Artificial Neural Network	Yes	Yes
		Error squared from visibility prediction, time	Nominal current consumption	i. Decision Trees ii. Discriminant Analysis iii. Naïve Bayes iv. Support Vector Machine v. Nearest Neighbor vi. Ensemble vii. Neural Network		

training data and performs poorly on new data. This highlights the need to find a balance between model complexity and performance on unseen data. Research by [22] indicates that overfitting in machine learning happens when the model

TABLE 2. Information regarding the meteorological parameters utilized in this study.

No	Features	Unit
1	Hourly visibility	Kilometer (km)
2	Hourly temperature	Degree Celsius (°C)
3	Hourly dew-point temperature	Degree Celsius (°C)
4	Hourly wind speed	Knot (kt)
5	Hourly wind direction	Degree (°)
6	Hourly relative humidity	Percentage (%)
7	Hourly pressure	Hectopascal (hPa)

TABLE 3. Nominal constant current regulator output current range.

Style	Current step	Nominal output (RMS Amperes)	Allowable range (RMS Amperes)
5-step CCR	5	6.60	6.50 - 6.70
	4	5.20	5.10 – 5.30
	3	4.10	4.00 – 4.30
	2	3.40	3.30 – 3.50
	1	2.80	2.70 – 2.90

fits the training data too closely, which reduces its ability to generalize. This is a widespread problem where further training improves the model's fitness on the training data, but its performance on unseen data decreases. Overfitting can harm the interpretability and generalizability of the resulting equations. A study by [23] shows that in Convolutional Neural Networks (CNN), overfitting occurs when the model performs well on the training data but fails to generalize to unseen data, resulting in lower accuracy. When training a CNN with limited samples, overfitting is often exacerbated, making it difficult for the model to effectively generalize.

Besides the k-fold approach, the Bayesian approach also helps reduce overfitting by considering the noise in the training data [22]. It guides the model's evolution towards an appropriate level of complexity based on the dataset. This leads to equations that are more suitable for the data, resulting in slight simplifications in the model form instead of overfitting. As a result, the model's generalizability and interpretability are enhanced [22]. The analysis of root mean square error demonstrates that regularization with Bayesian optimization effectively suppresses overfitting in the learning model [24]. This highlights the importance of proper model fitting. The Bayesian method is proven to be proficient in solving the overfitting issue, showcasing its ability to achieve accurate curve fitting while maintaining good generalization performance. By utilizing the Bayesian method, the cognitive abilities of machine learning are enhanced [24]. This demonstrates the practical implications of addressing overfitting in modeling tasks.

E. BAYESIAN OPTIMIZATION

One of the methods used to identify the most effective hyperparameter values in machine learning is the Bayesian approach [25], [26], [27]. The process begins by defining the variables: X represents the input data, Y is the target variable, and θ represents the model's hyperparameters. The main objective is to determine the values of θ that maximize the probability of the data given the model, P(Y|X, θ). The Bayesian approach starts with a prior distribution over θ, denoted as P(θ), which captures the initial beliefs about the likely ranges of hyperparameters before any data is observed. Then, using Bayes' rule, the target variables are updated based on the observed data [28];

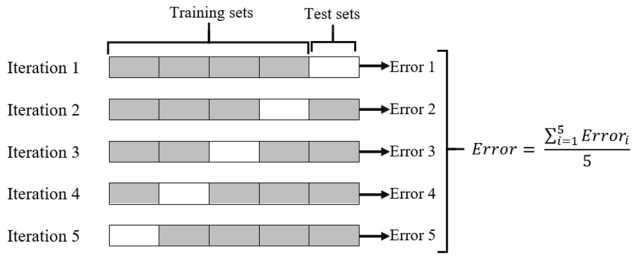

FIGURE 2. Example of cross fold validation with k = 5 ([20]).

$$P(\theta \mid X, Y) = P(Y \mid X, \theta) * \frac{P(\theta)}{P(Y, X)} \quad (1)$$

As shown in equation (1), P(θ |X,Y) represents the updated distribution over θ, which reflects new information about potential values of training hyperparameters given the data. P(Y|X, θ) indicates the probability of the data considering the training hyperparameters, reflecting how well the given set of hyperparameters fits the data. P(θ) is the prior distribution, encoding our beliefs about likely hyperparameter values before observing any data.

As for this study, the Bayesian optimization with acquisition function of expected improvement per second plus, iterations of 35 and false training time limit were used.

F. MODELLING FOR VISIBILITY PREDICTION

In this study, to predict the visibility error squared, five artificial intelligence models were compared to identify the optimal model based on meteorological conditions (Fig. 3). After conducting a preliminary evaluation using the Regression Learner in MATLAB R2023a software, Gaussian Process Regression (GPR) was selected as the first model (Model 1) among various algorithms. This choice was made because GPR yielded the lowest RMSE compared to other algorithms [29]. As described by [30] and [31] that used predefined settings optimized for specific data patterns and classification challenges, this study also uses the same approach where predefined settings in the regression learner model have been used. This comprehensive set of models significantly reduces the need for manual model optimization, streamlining the selection process and saving valuable time and effort in building and evaluating machine learning within MATLAB.

After the data is obtained from METAR, it must be cleaned first. The entire data set is checked for incorrect data entry,

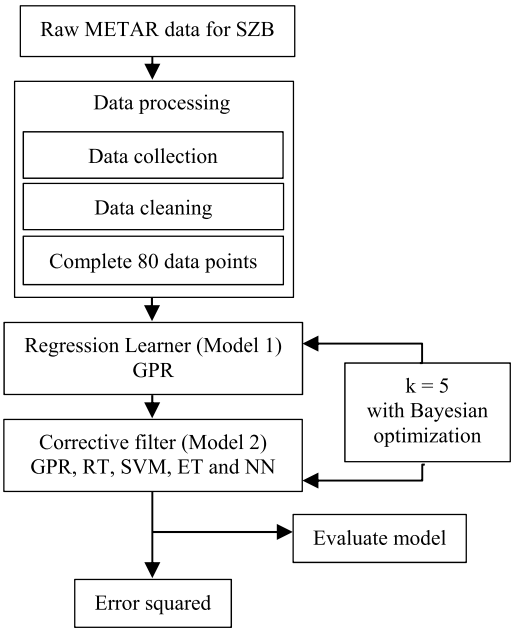

FIGURE 3. Flow chart showing the process used to obtained error squared.

inaccurate data, missing data, empty cells, and meaningless data compared to the raw METAR data. This process was conducted because the METAR data were manually separated into independent and dependent variables. The number of data points and features before and after cleaning the data set remains the same.

The search for optimized hyperparameters for the first model are shown in Table 4. The input data included temperature, dew point temperature, the difference between air temperature and dew point temperature, wind direction, wind speed, and pressure. The target output, on the other hand, is visibility. According to [32], applying an input lag time of 7 days usually yields the best results for most machine learning models and generalizes well across different subject areas. Therefore, for this study, a lag time of 3 days (from April 1st until April 3rd 2024), comprising of 80 data points with 480 input parameters were chosen.

The predicted visibility generated by GPR (Model 1) was used as an input to the second model, which is known as the correction filter (Model 2). The target output for both models is visibility. The correction filter utilized several models, including GPR, Regression Trees (RT), Support Vector Machines (SVM), Ensemble of Trees (ET), and Neural Networks (NN) [32]. These models were selected to improve the prediction capability of the regression learners [7], [10], [33], [34]. The hyperparameters for the correction filter are shown in Table 5. In this phase, the first model is stacked with the second model to predict visibility. The squared error from this model is then used, along with time, as input for the third model to classify the optimum nominal current consumption.

The following four statistical indicators, Mean Absolute Error (MAE), Mean Squared Error (MSE), Root Mean Squared Error (RMSE) and Coefficient of Determination (R^2) were utilized to evaluate the performance of the models (Equations (2) – (5)).

TABLE 4. GPR hyperparameters used as the first model.

Model Hyperparameters		
No	Features	Unit / Parameter
1	Signal standard deviation	0.79749
2	Optimize numeric parameters	Yes
Hyperparameter Search Range		
3	Sigma	0.0001 – 11.2783
4	Basic function	Constant, Zero, Linear
5	Kernel function	Nonisotropic Exponential, Nonisotropic Matern 3/2, Nonisotropic Matern 5/2, Nonisotropic Rational Quadratic, Nonisotropic Squared Exponential, Isotropic Exponential, Isotropic Matern 3/2, Isotropic Matern 5/2, Isotropic Rational Quadratic, Isotropic Squared Exponential,
6	Kernel scale	0.359 – 359
7	Standardize data	True, false

$$\text{MAE} = \frac{\sum_{i=1}^{n} |y_i - x_i|}{n} \tag{2}$$

$$\text{MSE} = \frac{1}{n}\sum_{i=1}^{n} (y_i - x_i)^2 \tag{3}$$

$$\text{RMSE} = \sqrt{\frac{1}{n}\sum_{i=1}^{n} (y_i - x_i)^2} \tag{4}$$

$$\text{R}^2 = 1 - \frac{\sum_{i=1}^{n} (y_i - x_i)^2}{\sum_{i=1}^{n} (y_i - \bar{x_i})^2} \tag{5}$$

where x_i is the actual visibility, y_i is the predicted visibility and n is the number of observations.

According to [7], evaluating the performance of a model often involves calculating the coefficient of determination (R^2). This metric measure how well the model can predict true visibility values on a scale from 0 to 1. An R^2 value of 1 indicates a perfect prediction, while 0 suggests no discernible relationship between the model's input and output. In addition to R^2, model accuracy is commonly assessed using MAE and RMSE. R^2 provides insights into precision, while MAE and RMSE measure the average differences and magnitude of these differences, respectively, between predictions and observations. When evaluating model performance, the following criteria are typically considered:

1) RMSE is always positive, and a smaller value indicates a more accurate model.
2) R^2 ranges from 0 to 1, with values closer to 1 indicating a well-performing model.
3) MSE is the square of RMSE, and a smaller MSE implies a successful model.
4) Similar to RMSE, MAE is positive, and a smaller value suggests a successful model. An error percentage close

TABLE 5. Model hyperparameters used as correction filter.

No	Features	Unit / Parameter
	GPR MODEL	
	Model Hyperparameters	
1	Signal standard deviation	0.79749
2	Optimize numeric parameters	Yes
	Hyperparameter Search Range	
3	Sigma	0.0001 – 11.2783
4	Basic function	Constant, Zero, Linear
5	Kernel function	Nonisotropic Exponential, Nonisotropic Matern 3/2, Nonisotropic Matern 5/2, Nonisotropic Rational Quadratic, Nonisotropic Squared Exponential, Isotropic Exponential, Isotropic Matern 3/2, Isotropic Matern 5/2, Isotropic Rational Quadratic, Isotropic Squared Exponential,
6	Kernel scale	0.005 – 5
7	Standardize data	True, false
	RT MODEL	
	Model Hyperparameters	
1	Surrogate decision splits	Off
	Hyperparameter Search Range	
2	Minimum leaf size	1 – 40
	SVM MODEL	
	Model Hyperparameters	
1	Kernel scale	1
	Hyperparameter Search Range	
2	Box constraint	0.001 – 1000
3	Kernel scale	0.001 – 1000
4	Epsilon	0.00074129 – 74.129
5	Kernel function	Gaussian, Linear, Quadratic, Cubic
6	Standardize data	True, false
	ET MODEL	
	Hyperparameter Search Range	
1	Ensemble method	Bag, LSBoost
2	Number of learners	10 – 500
3	Learning rate	0.001 – 1
4	Minimum leaf size	1 – 40
5	Number of predictors to sample	1 – 2
	NN MODEL	
	Model Hyperparameters	
1	Iteration limit	1000
	Hyperparameter Search Range	
2	Number of fully connected layers	1 – 3
3	Activation	ReLU, TanH, Sigmoid, None
4	Standardize data	Yes, no
5	First layer size	1 – 300
6	Second layer size	1 – 300
7	Third layer size	1 – 300
8	Regularization strength (Lambda)	1.25e-07 – 1250

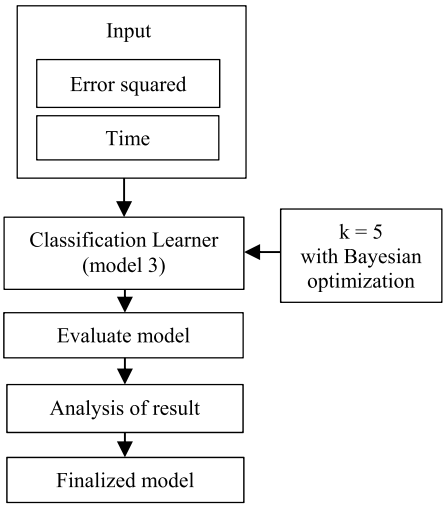

FIGURE 4. Flow chart showing the process used to obtained predicted current consumption for runway edge light.

to zero signifies that predicted values closely align with actual values.

G. MODELLING FOR NOMINAL OUTPUT CURRENT

The main objective of this study is to predict the nominal output current. As shown in Fig. 4, the input data for the models developed in this stage included the following parameters; time and error squared. The error squared represents the output from the visibility prediction modelling, while the time is obtained from the METAR data. The output is the nominal output current. For this stage, a total of 26 data points, gathered on October 4th 2023, with 52 input parameters, were used for training and validation. The data points consist of 7 observations of 3.4 A, 9 observations of 4.1 A, 7 observations of 5.2 A, and 3 observations of 6.6 A. The reason there is no data for 2.8 A is that the airport operates 24 hours a day, and the lights must be visible at all times. If the nominal current were set at 2.8 A, the lights would become almost invisible.

The software used for this analysis was MATLAB R2023a, and the Classification Learner was utilized. Using the same approach as [30] and [31] the models employed in this study included Decision Trees (DT), Discriminant Analysis (DA), Naïve Bayes Classifiers (NBC), SVM, Nearest Neighbor Classifiers (KNN), Ensemble Classifiers (EC), and Neural Network Classifiers (NNC) [35]. In this process, 20 % of the dataset was allocated for validation, while the remaining portion was used for training. This approach ensures that the models' performance is not biased by the training data [35]. In this phase, every cascaded model from the previous phase will be tested with each of the Classification Learner models.

The confusion matrix, also known as an error matrix, is a tool used in machine learning to evaluate the effectiveness of classification models. It is a summary table that shows how well the model has performed in predicting samples

TABLE 6. GPR optimized hyperparameters used as the first model.

Optimized Hyperparameters		
1	Basic function	Zero
2	Kernel function	Isotropic Exponential
3	Kernel scale	37.425
4	Sigma	0.00020804
5	Standardize data	Yes

from different classes. After analyzing the confusion matrix, various performance parameters, such as accuracy and area under the curve (AUC), are calculated to assess the model's performance. Accuracy is defined as the proportion of correct predictions out of all the predictions made. The AUC quantifies the model's ability to distinguish between different classes [35].

III. RESULTS AND DISCUSSION

A. MODELLING FOR VISIBILITY PREDICTION

Table 6 presents the results obtained from implementing the Regression Learner with Bayesian optimization. The first model, GPR, achieved MAE, MSE, RMSE, and R^2 values of 0.44391, 0.42288, 0.65029, and 0.67, respectively. This model was then combined with RT, SVM, GPR, NN, and ET to create the second model. The optimized hyperparameters used as correction filter is shown in Table 7 and the result for MAE, MSE, RMSE and R^2 is shown in Table 8.

In assessing the GPR model, the Nonisotropic Rational Quadratic yielded the best results with MAE, MSE, RMSE, and R^2 values of 0.11114, 0.097761, 0.31267, and 0.92, respectively. In evaluating the RT model, the best performance was achieved with a minimum leaf size of 5, resulting in MAE, MSE, RMSE, and R^2 values of 0.23393, 0.30409, 0.55145, and 0.76. For the SVM model, based on performance, the Linear function was found to be the most suitable choice, producing MAE, MSE, RMSE, and R^2 values of 0.088952, 0.087573, 0.29593, and 0.93, respectively. Subsequently, for the ET model, LSBoost was selected as the superior technique based on accuracy, achieving MAE, MSE, RMSE, and R^2 values of 0.21393, 0.17311, 0.41607, and 0.86, respectively. Finally, regarding NN, None was found to be the best activation function, resulting in MAE, MSE, RMSE, and R^2 values of 0.10388, 0.092309, 0.30382, and 0.93.

B. MODELLING FOR NOMINAL OUTPUT CURRENT

To determine the most suitable model for predicting the nominal output current based on error squared and time, the best models among DT, DA, NBC, SVM, KNN, EC and NNC models were determined first. To determine the optimal internal structure of each model, various internal parameters were set to assess the accuracy level. The model with the highest accuracy was identified as the best-fit model. Owing to the number of iterations performed to achieve the best model, the results of each step involved are not provided. However, Table 9 showcases the results obtained from the best-fit model for every cascaded model. The combination of GPR, GPR, KNN achieved the highest accuracy of 96.2 %. On the other hand, the combination of GPR, RT, SVM was the least accurate with an accuracy of 88.5 %.

TABLE 7. Optimized hyperparameters used as correction filter.

GPR MODEL		
Optimized Hyperparameters		
1	Basic function	Linear
2	Kernel function	Nonisotropic Rational Quadratic
3	Kernel scale	0.26219
4	Sigma	0.00010285
5	Standardize data	No
RT MODEL		
Optimized Hyperparameters		
1	Minimum leaf size	5
SVM MODEL		
Optimized Hyperparameters		
1	Kernel function	Linear
2	Box constraint	14.1927
3	Epsilon	0.0031914
4	Standardize data	Yes
ET MODEL		
Optimized Hyperparameters		
1	Ensemble method	LSBoost
2	Minimum leaf size	1
3	Number of learners	10
4	Learning rate	0.3719
5	Number of predictors to sample	1
NN MODEL		
Optimized Hyperparameters		
1	Number of fully connected layers	1
2	Activation	None
3	Standardize data	No
4	First layer size	6
5	Regularization strength (Lambda)	1.4549e-07

TABLE 8. Result for MAE, MSE, RMSE and R^2 for model 1 and model 2.

	Regression Learner	MAE	MSE	RMSE	R^2
Model 1	GPR	0.44391	0.42288	0.65029	0.67
Model 2	RT	0.23393	0.30409	0.55145	0.76
	SVM	0.088952	0.087573	0.29593	0.93
	GPR	0.11114	0.097761	0.31267	0.92
	NN	0.10388	0.092309	0.30382	0.93
	ET	0.21393	0.17311	0.41607	0.86

TABLE 9. Result for best-fit model.

Regression Learner		Classification Learner	True predicted	False predicted	Acc. (%)
Model 1	Model 2	Model 3			
	RT	SVM	23	3	88.5
	SVM	KNN	24	2	92.3
GPR	GPR	KNN	25	1	96.2
	NN	KNN	24	2	92.3
	ET	KNN	24	2	92.3

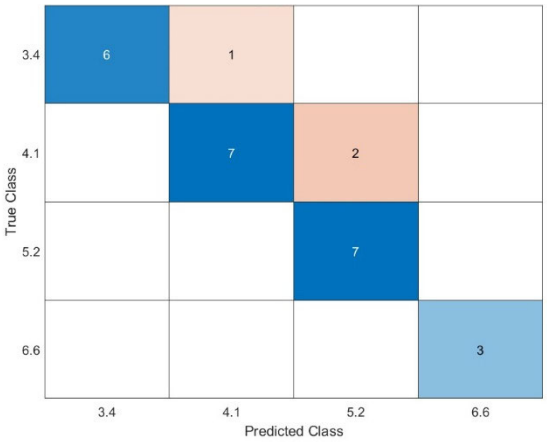

FIGURE 5. Confusion matrix for GPR, RT and SVM model combination.

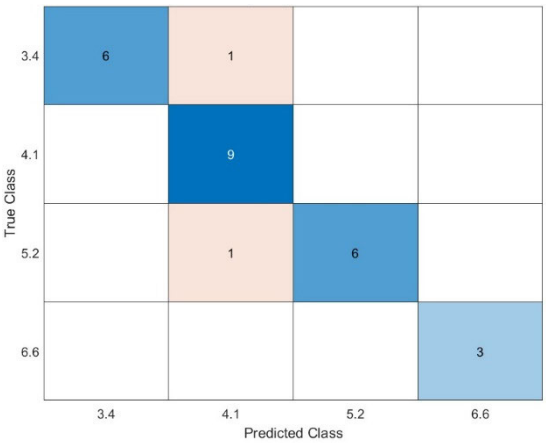

FIGURE 6. Confusion matrix for GPR, SVM and KNN model combination.

Fig. 5 to Fig. 9 illustrate the confusion matrices used to evaluate the performance of DT, DA, NBC, SVM, KNN, EC, and NNC models in forecasting the nominal output current. The x-axis represents the predicted class, showing the values predicted by the respective models. The y-axis represents the true class, indicating the actual values used at the airport. The numerical values 3.4 A, 4.1 A, 5.2 A, and 6.6 A represent the nominal current output. Values successfully predicted by the respective model are shown in blue, while inaccurately predicted values are shown in orange. The cumulative number of predictions amounts to 26.

For example, in Fig. 5, there are 6 instances where the predicted data is exactly 3.4 A, 7 instances where the predicted data is exactly 4.1 A, 7 instances where the predicted data is exactly 5.2 A and 3 instances where the predicted data is exactly 6.6 A. However, there is 1 case where the model inaccurately predicted 4.1 A, and 2 cases where the model inaccurately predicted 5.2 A. Therefore, cumulatively, there are a total of 26 predictions.

Based on these findings, it can be concluded that KNN is the most accurate model for classification purposes. This model has outperformed other models in classifying the nominal current output.

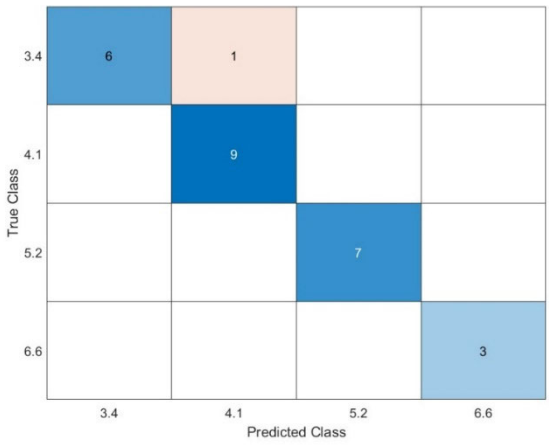

FIGURE 7. Confusion matrix for GPR, GPR and KNN model combination.

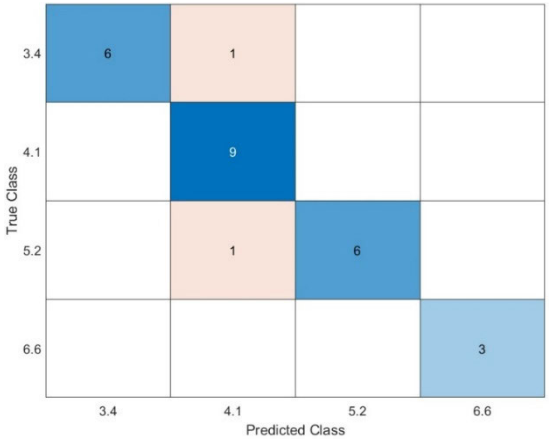

FIGURE 8. Confusion matrix for GPR, NN and KNN model combination.

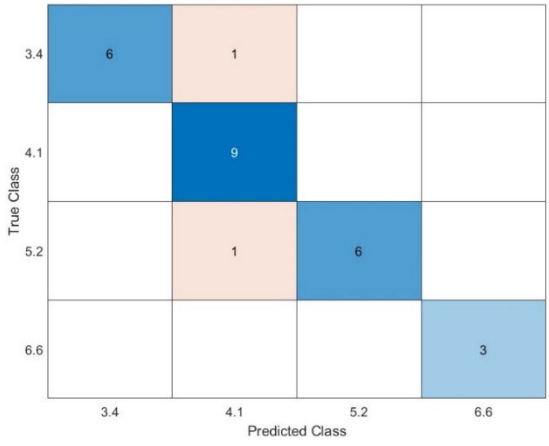

FIGURE 9. Confusion matrix for GPR, ET and KNN model combination.

TABLE 10. Result for implementing the models at actual airport operation.

Model combination			Accuracy (%)	Improve and equal prediction (%)
Model 1	Model 2	Model 3		
GPR	RT	SVM	88.5	91.85
GPR	SVM	KNN	92.3	91.85
GPR	GPR	KNN	96.2	91.85
GPR	NN	KNN	92.3	91.85
GPR	ET	KNN	92.3	91.85

TABLE 11. AUC result for all models.

Models	AUC for Nominal Output Current (A)			
	3.4	4.1	5.2	6.6
GPR, RT, SVM	0.9774	0.8824	0.9699	1
GPR, SVM, KNN	0.9286	0.9412	0.9286	1
GPR, GPR, KNN	0.8759	0.9575	1	1
GPR, NN, KNN	0.8797	0.9542	0.985	1
GPR, ET, KNN	0.8797	0.9542	0.985	1

To further evaluate the success of the models in predicting or improving the nominal output current, a selected combination of models was tested from October 5th, 2023 to October 10th, 2023 during actual airport operations. The total number of data points were 135 that consists of time and error squared for each data points. The results of this test, as shown in Table 10, indicate that the models have successfully achieved a 91.85 % accuracy rate in predicting the same or improved nominal output current.

The concept of ''improved nominal output current'' in the context of constant current regulators (CCRs) refers to the model's ability to optimize the output current settings based on specific operational conditions. In standard practice, CCRs are set to a nominal current value, such as 6.6 A, which is presumed to be adequate under typical conditions. This setting ensures that lighting systems operate within the desired parameters, providing sufficient illumination for safe airport operations. However, the model is able to predict an optimized nominal output current that is more suitable for current operational conditions. For instance, instead of maintaining a constant 6.6 A, the model may determine that a setting of 5.2 A is sufficient for the prevailing conditions.

Fig. 10 to Fig. 14 depict the receiver operating characteristic (ROC) curves and the corresponding area under them. The ROC curve illustrates the relationship between the true positive rate (TPR) and the false positive rate (FPR) at various thresholds for classification scores, which are calculated by the currently selected classifier. The Model Operating Point displays the false positive rate and true positive rate that correspond to the threshold utilized by the classifier for classifying an observation.

The AUC value, shown in Table 11, is a measure of the overall quality of the classifier. The AUC values are in the range 0 to 1 and larger AUC values indicate better classifier performance. For a nominal output current of 3.4 A, the combination of GPR, RT and SVM achieves the highest AUC of 0.9774. This indicates excellent model

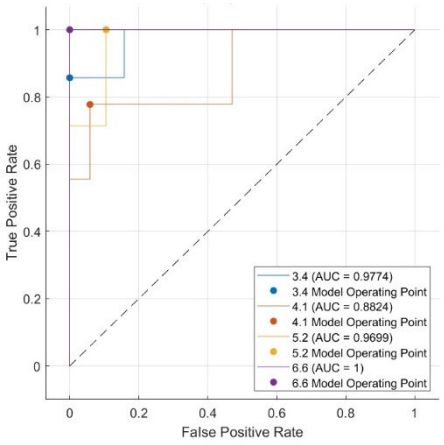

FIGURE 10. AUC for GPR, RT and SVM.

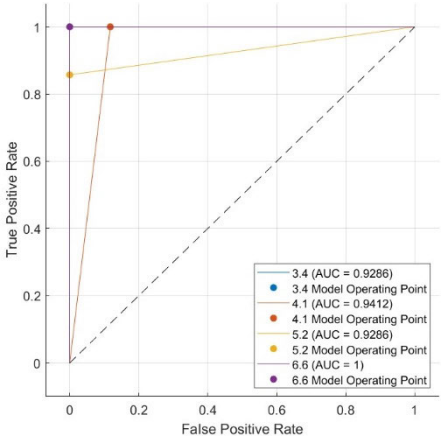

FIGURE 11. AUC for GPR, SVM and KNN.

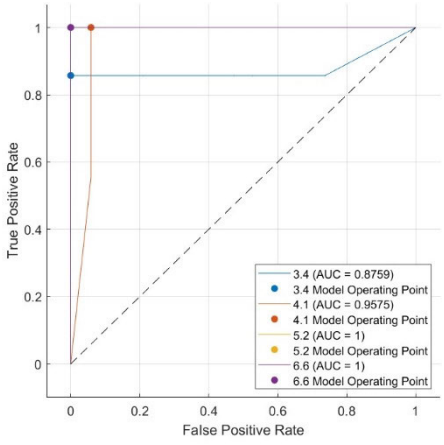

FIGURE 12. AUC for GPR, GPR and KNN.

performance with nearly perfect classification ability. Other model combinations, such as GPR, SVM, KNN and GPR, GPR, KNN, also perform reasonably well with AUC values of 0.9286 and 0.8759, respectively. However, combinations of GPR, NN, KNN and GPR, ET, KNN show slightly lower AUC values of 0.8797 each. This suggests that while GPR, RT, SVM models collectively offer the highest predictive accuracy for 3.4 A, NN and ET could still provide viable alternatives with slight trade-offs in performance.

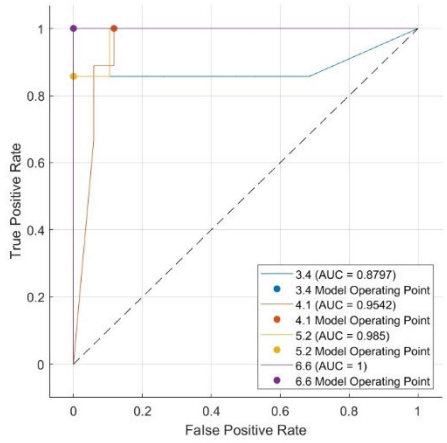

FIGURE 13. AUC for GPR, NN and KNN.

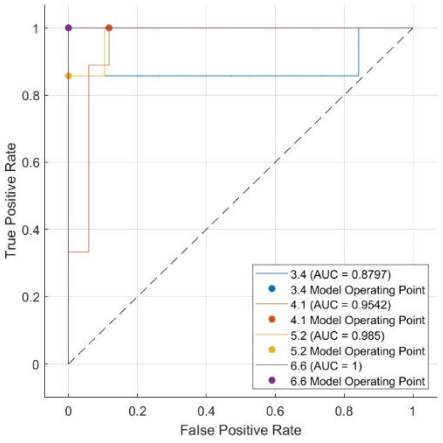

FIGURE 14. AUC for GPR, ET and KNN.

At a nominal output current of 4.1 A, the combination of GPR, GPR, KNN achieves the highest AUC of 0.9575. This suggests that it has a strong predictive capability at this current level, surpassing other combinations. Interestingly, both GPR, SVM, KNN and GPR, NN, KNN also achieve high AUC values of 0.9412 and 0.9542, respectively, indicating consistent performance across these models. The combination of GPR, RT, SVM shows a relatively lower AUC of 0.8824, which may suggest a slight decrease in the effectiveness of the model for this specific current. However, this decrease is still within an acceptable range, indicating satisfactory performance.

When the nominal output current is increased to 5.2 A, the combination of GPR, GPR, KNN achieves a perfect AUC score of 1. This suggests flawless classification capability for this current setting. Similarly, the combination of GPR, RT, SVM also yields a near-perfect AUC of 0.9699, highlighting its robustness. The GPR, NN, KNN and GPR, ET, KNN combinations show very high AUC values of 0.985, indicating excellent predictive performance. These results underscore that for 5.2 A, GPR combined with any of the other models provides superior predictive accuracy.

For a nominal output current of 6.6 A, all model combinations achieve a perfect AUC score of 1. This indicates that all tested combinations are equally capable of perfectly distinguishing the classes at this current level. The universality of this result suggests that at higher currents, the predictive models reach an optimal performance plateau, potentially due to clearer differentiation between the classes.

In terms of model combination, GPR, RT, SVM exhibits superior performance at 3.4 A. However, it slightly underperforms at 4.1 A compared to other combinations. It does, however, have near-perfect or perfect performance at 5.2 A and 6.6 A. GPR, SVM, KNN performs consistently well across all current levels. It is particularly strong at 4.1 A. GPR, GPR, KNN achieves the highest AUC at 4.1 A and is perfect at 5.2 A and 6.6 A. This shows that the model is reliable and has robust performance, demonstrating the efficacy of combining GPR models. GPR, NN, KNN and GPR, ET, KNN show remarkable consistency and high AUC values across all current levels, while having a perfect AUC at 6.6 A indicates robustness at higher current levels.

This analysis shows that GPR-based model combinations generally provide robust and high-performing solutions across various nominal output currents. The combination of GPR, RT and SVM stands out at 3.4 A, while GPR, GPR, KNN demonstrates exceptional performance at 4.1 A, 5.2 A and 6.6 A. The inclusion of NN and ET also contributes to high performance, suggesting their potential integration in predictive modeling for nominal output currents. This detailed evaluation highlights the importance of selecting appropriate model combinations tailored to specific current settings to achieve optimal nominal current output accuracy.

Overall, this supports the findings of this study that the combination of GPR, GPR, KNN produced the best accuracy for optimum nominal current output based on error squared and time.

IV. CONCLUSION

In this study, to determine the best model for the prediction of nominal current output based on meteorological parameters and time at Subang Airport, five Regression Learner models that consists of Gaussian Process Regression (GPR), Regression Tress (RT), Support Vector Machines (SVM), Ensemble of Trees (ET) and Neural Networks (NN) and seven Classification Learner models such as Decision Tress (DT), Discriminant Analysis (DA), Naïve Bayes Classifiers (NBC), Support Vector Machines (SVM), Nearest Neighbor Classifiers (KNN), Ensemble Classifiers (EC) and Neural Network Classifiers (NN) were applied and their accuracy was compared.

Meteorological factors, including time, daily air temperature, dew point temperature, difference between air temperature and dew point temperature, wind direction, wind speed and pressure, are used for calculation and screening. The performance of classification models in machine learning was analyzed using a confusion matrix. Accuracy and area under the curve (AUC), were calculated based on the obtained confusion matrix to evaluate the models' performance. The combination of GPR, GPR, KNN algorithm

achieved the highest accuracy of 96.2 %. The accuracy is aligned with the AUC of the model, having the highest value compared to other models. Therefore, according to the results, the GPR, GPR, KNN model was the most suitable model for the prediction of nominal current output. Eventually, by introducing the model to predict the nominal current output during actual airport operation, the model can predict the actual and improved nominal current output by 91.85 %.

In conclusion, this study has achieved its novelty by improving visibility prediction using an optimum correction filter, classifying the optimum nominal current output by harnessing the error produced by regression models, and providing a robust model with optimum performance and high accuracy for predicting nominal current output. As a recommendation, it is suggested that this study be expanded to incorporate other types of lighting systems so that regulators and airport operators can have a comprehensive model for the entire aeronautical ground lighting system at different airports, which may have diverse configurations, settings, and operations.

ACKNOWLEDGMENT

The authors would like to thank the Public Service Department of Malaysia and the Civil Aviation Authority of Malaysia and also would like to thank the local airport operator for their support and participation in this study.

DECLARATION OF GENERATIVE AI AND AI-ASSISTED TECHNOLOGIES IN THE WRITING PROCESS

During the preparation of this work the author(s) used editGPT to improve language and understanding. After using this tool/service, the author(s) reviewed and edited the content as needed and take(s) full responsibility for the content of the publication.

REFERENCES

[1] *Intensity Control of Approach and Runway Lights in Aerodrome Design and Operations*, 9th ed., Int. Civil Aviation Org. (ICAO), Montreal, QC, Canada, 2022.

[2] *Light Intensity Settings in Aerodrome Design Manual Part 4: Visual Aids*, 5th ed., Int. Civil Aviation Org. (ICAO), Montreal, QC, Canada, 2021, pp. 1–5.

[3] G. Wei, Z. Zhang, X. Ouyang, Y. Shen, S. Jiang, B. Liu, and B.-J. He, "Delineating the spatial–temporal variation of air pollution with urbanization in the belt and road initiative area," *Environ. Impact Assessment Rev.*, vol. 91, Nov. 2021, Art. no. 106646, doi: 10.1016/j.eiar.2021.106646.

[4] D. Liu, T. Jiang, Y. Zhang, Y. Wang, X. Pan, and J. Wu, "Forecast model of airport haze visibility and meteorological factors based on SVR-RBF model," *IOP Conf. Ser., Earth Environ. Sci.*, vol. 657, no. 1, Feb. 2021, Art. no. 012029, doi: 10.1088/1755-1315/657/1/012029.

[5] P. Kneringer, S. J. Dietz, G. J. Mayr, and A. Zeileis, "Probabilistic nowcasting of low-visibility procedure states at Vienna international airport during cold season," *Pure Appl. Geophys.*, vol. 176, no. 5, pp. 2165–2177, May 2019, doi: 10.1007/s00024-018-1863-4.

[6] J. Ding, G. Zhang, S. Wang, B. Xue, J. Yang, J. Gao, K. Wang, R. Jiang, and X. Zhu, "Forecast of hourly airport visibility based on artificial intelligence methods," *Atmosphere*, vol. 13, no. 1, p. 75, Jan. 2022, doi: 10.3390/atmos13010075.

[7] N. Penov and G. Guerova, "Sofia airport visibility estimation with two machine-learning techniques," *Remote Sens.*, vol. 15, no. 19, p. 4799, Oct. 2023, doi: 10.3390/rs15194799.

[8] C. Peláez-Rodríguez, C. M. Marina, J. Pérez-Aracil, C. Casanova-Mateo, and S. Salcedo-Sanz, "Extreme low-visibility events prediction based on inductive and evolutionary decision rules: An explicability-based approach," *Atmosphere*, vol. 14, no. 3, p. 542, Mar. 2023, doi: 10.3390/atmos14030542.

[9] P. W. Chan, W. Wen, and L. Li, "Research on the usability of different machine learning methods in visibility forecasting," *Atmósfera*, vol. 37, pp. 99–111, Dec. 2023, doi: 10.20937/atm.53053.

[10] A. Shankar and B. C. Sahana, "Early warning of low visibility using the ensembling of machine learning approaches for aviation services at Jay Prakash Narayan International (JPNI) airport Patna," *Social Netw. Appl. Sci.*, vol. 5, no. 5, May 2023, doi: 10.1007/s42452-023-05350-7.

[11] S. M. Mirou, A. T. Elawady, A. G. Ashour, W. Zeiada, and M. Abuzwidah, "Visibility prediction through machine learning: Exploring the role of meteorological factors," in *Proc. Adv. Sci. Eng. Technol. Int. Conf. (ASET)*, Feb. 2023, pp. 1–6, doi: 10.1109/aset56582.2023.10180539.

[12] Y. Zhang, Y. Wang, Y. Zhu, L. Yang, L. Ge, and C. Luo, "Visibility prediction based on machine learning algorithms," *Atmosphere*, vol. 13, no. 7, p. 1125, Jul. 2022, doi: 10.3390/atmos13071125.

[13] S. Cornejo-Bueno, D. Casillas-Pérez, L. Cornejo-Bueno, M. I. Chidean, A. J. Caamaño, J. Sanz-Justo, C. Casanova-Mateo, and S. Salcedo-Sanz, "Persistence analysis and prediction of low-visibility events at valladolid airport, Spain," *Symmetry*, vol. 12, no. 6, p. 1045, Jun. 2020, doi: 10.3390/sym12061045.

[14] W. Choi, J. Park, D. Kim, J. Park, S. Kim, and H. Lee, "Development of two-dimensional visibility estimation model using machine learning: Preliminary results for South Korea," *Atmosphere*, vol. 13, no. 8, p. 1233, Aug. 2022, doi: 10.3390/atmos13081233.

[15] B. Li, W. Zhang, Z. Li, and B. Guo, "Research on application of LED navaid lighting in airfield area of civil airports," *IOP Conf. Ser. Mater. Sci. Eng.*, vol. 392, no. 1, 2018, doi: 10.1088/1757-899X/392/6/062109.

[16] *Aviation Weather Center*. Accessed: Apr. 1, 2023. [Online]. Available: https://aviationweather.gov/data/metar/

[17] *Rating Characteristics of Constant Current Regulators in Aerodrome Design Manual Part 5: Electrical System*, 2nd ed., Int. Civil Aviation Org. (ICAO), Montreal, QC, Canada, 2017, pp. 7–8.

[18] F. M. Cordeiro, G. B. França, F. L. de Albuquerque Neto, and I. Gultepe, "Visibility and ceiling nowcasting using artificial intelligence techniques for aviation applications," *Atmosphere*, vol. 12, no. 12, p. 1657, Dec. 2021, doi: 10.3390/atmos12121657.

[19] P. K. Kanti, P. Sharma, B. Koneru, P. Banerjee, and K. D. Jayan, "Thermophysical profile of graphene oxide and MXene hybrid nanofluids for sustainable energy applications: Model prediction with a Bayesian optimized neural network with K-cross fold validation," *FlatChem*, vol. 39, May 2023, Art. no. 100501, doi: 10.1016/j.flatc.2023.100501.

[20] H. L. Vu, K. T. W. Ng, A. Richter, and C. An, "Analysis of input set characteristics and variances on k-fold cross validation for a recurrent neural network model on waste disposal rate estimation," *J. Environ. Manage.*, vol. 311, Jun. 2022, Art. no. 114869, doi: 10.1016/j.jenvman.2022.114869.

[21] H. Li, J. Li, X. Guan, B. Liang, Y. Lai, and X. Luo, "Research on overfitting of deep learning," in *Proc. 15th Int. Conf. Comput. Intell. Secur. (CIS)*, 2019, pp. 78–81, doi: 10.1109/CIS.2019.00025.

[22] G. F. Bomarito, P. E. Leser, N. C. M. Strauss, K. M. Garbrecht, and J. D. Hochhalter, "Bayesian model selection for reducing bloat and overfitting in genetic programming for symbolic regression," in *Proc. GECCO Companion*, 2022, pp. 526–529, doi: 10.1145/3520304.3528899.

[23] P. Thanapol, K. Lavangnananda, P. Bouvry, F. Pinel, and F. Leprévost, "Reducing overfitting and improving generalization in training convolutional neural network (CNN) under limited sample sizes in image recognition," in *Proc. 5th Int. Conf. Inf. Technol. (InCIT)*, Oct. 2020, pp. 300–305, doi: 10.1109/InCIT50588.2020.9310787.

[24] C. Bu and Z. Zhang, "Research on curve fitting and overfitting based on Bayesian method," in *Proc. 6th Int. Symp. Comput. Inf. Process. Technol. (ISCIPT)*, Jun. 2021, pp. 141–144, doi: 10.1109/ISCIPT53667.2021.00035.

[25] M. Aghaabbasi, M. Ali, M. Jasinski, Z. Leonowicz, and T. Novák, "On hyperparameter optimization of machine learning methods using a Bayesian optimization algorithm to predict work travel mode choice," *IEEE Access*, vol. 11, pp. 19762–19774, 2023, doi: 10.1109/ACCESS.2023.3247448.

[26] B. Bischl, M. Binder, M. Lang, T. Pielok, J. Richter, S. Coors, J. Thomas, T. Ullmann, M. Becker, A. Boulesteix, D. Deng, and M. Lindauer, "Hyperparameter optimization: Foundations, algorithms, best practices, and open challenges," *WIREs Data Mining Knowl. Discovery*, vol. 13, no. 2, p. e1484, Mar. 2023, doi: 10.1002/widm.1484.

[27] H.-T. Vo, H. T. Ngoc, and L.-D. Quach, "An approach to hyperparameter tuning in transfer learning for driver drowsiness detection based on Bayesian optimization and random search," *Int. J. Adv. Comput. Sci. Appl.*, vol. 14, no. 4, pp. 828–837, 2023, doi: 10.14569/ijacsa.2023.0140492.

[28] M. Alruqi, P. Sharma, and Ü. Ağbulut, "Investigations on biomass gasification derived producer gas and algal biodiesel to power a dual-fuel engines: Application of neural networks optimized with Bayesian approach and K-cross fold," *Energy*, vol. 282, Nov. 2023, Art. no. 128336, doi: 10.1016/j.energy.2023.128336.

[29] W. M. R. B. Jamaludin, W. M. B. W. Mohamed, N. H. B. N. Ali, and N. A. B. M. Isa, "Utilizing advanced regression techniques to forecast visibility at Subang and Langkawi international airport," in *Proc. New Trends Civil Aviation (NTCA)*, Apr. 2024, pp. 185–190, doi: 10.23919/ntca60572.2024.10517824.

[30] M. Zubair and Y. Akram, "Utilizing MATLAB machine learning models to categorize transient events in a nuclear power plant using generic pressurized water reactor simulator," *Nucl. Eng. Design*, vol. 415, Dec. 2023, Art. no. 112698, doi: 10.1016/j.nucengdes.2023.112698.

[31] M. Zubair and Y. Akram, "Enhancement in the safety and reliability of pressurized water reactors using machine learning approach," *Ann. Nucl. Energy*, vol. 201, Jun. 2024, Art. no. 110448, doi: 10.1016/j.anucene.2024.110448.

[32] N. A. Hazrin, K. L. Chong, Y. F. Huang, A. N. Ahmed, J. L. Ng, C. H. Koo, K. W. Tan, M. Sherif, and A. El-shafie, "Predicting sea levels using ML algorithms in selected locations along coastal Malaysia," *Heliyon*, vol. 9, no. 9, Sep. 2023, Art. no. e19426, doi: 10.1016/j.heliyon.2023.e19426.

[33] M. Zhen, M. Yi, T. Luo, F. Wang, K. Yang, X. Ma, S. Cui, and X. Li, "Application of a fusion model based on machine learning in visibility prediction," *Remote Sens.*, vol. 15, no. 5, p. 1450, Mar. 2023, doi: 10.3390/rs15051450.

[34] C. Peláez-Rodríguez, J. Pérez-Aracil, A. de Lopez-Diz, C. Casanova-Mateo, D. Fister, S. Jiménez-Fernández, and S. Salcedo-Sanz, "Deep learning ensembles for accurate fog-related low-visibility events forecasting," *Neurocomputing*, vol. 549, Sep. 2023, Art. no. 126435, doi: 10.1016/j.neucom.2023.126435.

[35] F. Mohammadi, H. Teiri, Y. Hajizadeh, A. Abdolahnejad, and A. Ebrahimi, "Prediction of atmospheric $PM_{2.5}$ level by machine learning techniques in Isfahan, Iran," *Sci. Rep.*, vol. 14, no. 1, pp. 1–12, Jan. 2024, doi: 10.1038/s41598-024-52617-z.

W. M. R. JAMALUDIN was born in Penang, Malaysia, in 1980. He received the Diploma degree in electrical engineering (instrumentation) and the degree (Hons.) in electrical engineering from Universiti Teknologi MARA (UiTM) Shah Alam, in 2001 and 2004, respectively, and the master's degree in communication and computer engineering from Universiti Kebangsaan Malaysia (UKM) Bangi, in 2015. He is currently pursuing the Ph.D. degree in mechanical engineering with UiTM Shah Alam.

From 2006 to 2015, he was attached with Public Works of Malaysia and appointed as an Electrical Engineer working on various government projects. In 2015, he joined Civil Aviation Authority of Malaysia (CAAM) as the Principal Assistant Director. His research interests include aeronautical ground light (AGL), airport control and lighting monitoring systems (ACLMS), and airport electrical systems.

Mr. Jamaludin is also a Graduate Member of the Board of Engineers Malaysia (BEM) and a Professional Technologists registered with Malaysia Board of Technologist (MBOT) in Electrical and Electronics Technology.

N. H. NIK ALI (Senior Member, IEEE) was born in Malaysia, in 1990. He received the B.Eng. degree (Hons.) in electrical power engineering from Universiti Tenaga Nasional (UNITEN), Malaysia, in 2013, and the Ph.D. degree in electronics and electrical engineering from the University of Southampton, U.K., in 2017.

He was a Research Fellow with the School of Electronics and Computer Science, University of Southampton, from 2018 to 2019. He was a Postdoctoral Researcher with the Institute of Power Engineering (IPE), UNITEN, from 2019 to 2020. Currently, he is a Senior Lecturer with Universiti Teknologi MARA (UiTM) Shah Alam, Malaysia. His research interests include condition monitoring of high-voltage cables and transformers, partial discharge measurement, HV insulation/dielectric materials, transformer rating analysis, lightning analysis, sustainable energy management, electric vehicle supply equipment (EVSE), and any applications related to applied signal processing.

Dr. Nik Ali is also a Graduate Member of the Board of Engineers Malaysia (BEM) and a Professional Technologists registered with Malaysia Board of Technologist (MBOT).

W. M. WAN MOHAMED received the degree in aerospace engineering and in aircraft maintenance engineering from St. Louis University, USA, in 1989, the M.Sc. degree in air transport management from Cranfield University, U.K., in 1998, and the Ph.D. degree from UiTM, Malaysia, in 2016.

She started her career as an Aircraft Planning Engineer with Airod Sdn Bhd, in 1989, and her last post was as the Technical Training Manager (1995–1997). She has more than 25 years of experience as an Academician. She joined Universiti Sains Malaysia (USM) as a Senior Lecturer and was later promoted to the Deputy Dean of Postgraduate and Research with the School of Aerospace Engineering, USM. She joined the Department of Mechanical Engineering, UNITEN, as a Senior Lecturer, in 2001, and the Faculty of Mechanical Engineering, UiTM Shah Alam, in 2003, as a Senior Lecturer.

Dr. Wan Mohamed is also appointed as one of the Technical Committee Member of Ministry of Transport (MOT) involved in the Development of Malaysia Transport Policy (Aviation Sector), Malaysia 12th Plan (RMK-12), Sustainable Railway Development Framework, an Advisor to Technology Depository Agency (TDA) Malaysia for Aviation Sector, and a Technical Committee Member of the Department of Standards Malaysia in developing the Vehicle Aftermarket—Service, Spare Parts, Sales & Smash Repair (4S) Standards, and a Technical Evaluator for Ministry of Human Resource Malaysia in evaluating the Occupational Framework for Air Transportation Sector. Currently, she is one of the consultants appointed by MOT to develop the National Airport Strategic Planning (NASP) and a Cabinet Committee Member in mitigating traffic safety and congestion in Malaysia.

N. A. M. ISA was born in Ipoh, Malaysia, in 1975. She received the B.Eng. degree (Hons.) in civil engineering from the University of Malaya, the master's Diploma degree in airport engineering management from the National University of Singapore, the Master of Business Administration degree from Universiti Utara Malaysia, and the Doctor of Business Administration degree from UiTM.

She joined Malaysia Airports, in 2002, as a Civil Engineer. She was the General Manager of Planning and Development, in 2011, and the Head of Engineering with MA (Sepang), in 2016. She left Malaysia Airports, in 2018, to broaden her aviation experience and rejoined, in February 2021, as the Head of Technical Services, until May 2024.

Dr. Isa has been accredited as an International Airport Professional, since 2011. She is currently representing Malaysia Airports in the ACI Asia–Pacific & Middle East Regional Environment Committee. She is also a certified Project Management Professional.